Ironless wheel motor for a direct drive vehicle application

M.C. Greaves, A.G. Simpson, B.D. Guymer, Dr G.R. Walker & D.A. Finn

Sustainable Energy Research Group (SERG)
School of Information Technology and Electrical Engineering
University of Queensland

Abstract
An ironless motor for use as direct wheel drive is presented. The motor is intended for use in a lightweight (600kg), low drag, series hybrid commuter vehicle under development at The University of Queensland. The vehicle will utilise these ironless motors in each of its rear wheels, with each motor producing a peak torque output of 500Nm and a maximum rotational speed of 1500rpm. The axial flux motor consists of twin Ironless litz wire stators with a central magnetic ring and simplified Halbach magnet arrays on either side. A small amount of iron is used to support the outer Halbach arrays and to improve the peak magnetic flux density. Ducted air cooling is used to remove heat from the motor and will allow for a continuous torque rating of 250Nm.

Ironless machines have previously been shown to be effective in high speed, high frequency applications (+1000Hz). They are generally regarded as non-optimal for low speed applications as iron cores allow for better magnet utilisation and do not significantly increase the weight of a machine. However, ironless machines can also be seen to be effective in applications where the average torque requirement is much lower than the peak torque requirement such as in some vehicle drive applications. The low spinning losses in ironless machines are shown to result in very high energy throughput efficiency in a wide range of vehicle driving cycles.

List of Symbols

B_{peak} = Magnetic Flux Density (T)
J_{rms} & J_{peak} =RMS & Peak Current Density (A/m^2)
r = Average winding radius (m)
R_{outer} = Outer winding radius in magnetic field (m)
R_{inner} = Inner winding radius in magnetic field (m)
$t_{thickness}$ =Thickness of stator (purely copper) (m)
D =Nominal Wire Diameter (m)
$D_{insulated}$ = Insulated Wire Diameter (m)
$N_{Conductors}$ = Total number of individual conductors
K_{ends} = Increase in turn length due to end turns
V_{active} = Active volume of copper (m^3)
r = Resistivity of Copper **(Ωm)**

1. INTRODUCTION

The level of urban air pollution, global warming due to greenhouse gas production and the current rate of oil consumption are driving a revolution in automotive propulsion technologies. In recent years there has been an introduction of hybrid electric vehicles by major automotive companies; including the Honda Insight and the Toyota Prius. These hybrid vehicles can provide a significant reduction in emission and fuel consumption, but they are only an intermediate solution to sustainable personal transportation.

2. HYPERCARS and the ULTRACOMMUTER

A Hypercar[tm] is a vehicle concept proposed by the Rocky Mountain Institute [1] to dramatically increase vehicle efficiency without significantly increasing the vehicle's cost. The concept proposes a large reduction in both vehicle mass and aerodynamic drag. The resulting lower power required to drive the vehicle will result in a smaller, lighter drive train, which then further reduces the mass of the vehicle. This concept of mass decompounding and ultra low drag combined with low power accessories and highly efficient hybrid electric drive train is shown to result in a family vehicle with a fuel consumption of between 1-2 L/100km. The University of Queensland has recently undertaken the design and development of a two-seater commuter vehicle that utilises the concept behind the Hypercar and has named the vehicle the UltraCommuter [2, 3].

Fig.1: The UltraCommuter Concept

3. DRIVE EFFICIENCY CONSIDERATIONS

In many industrial applications motors often operate under near constant conditions close to their maximum efficiency point. In automotive applications the drive-train operates under constantly varying torques and speeds. For this reason the selection of a motor should not just be based on its maximum efficiency point, but rather on the overall cycle efficiency under typical driving conditions. When considering various standard driving cycles [4] such as the Air Resources board No.2 (ARB02), the Urban Dynamometer driving cycle (UDDS) and the Highway Fuel economy test (HWFET) it can be seen through histogram analysis that by far the largest energy throughput for the UltraCommuter is at low torque average speed operation and not in high torque operation.

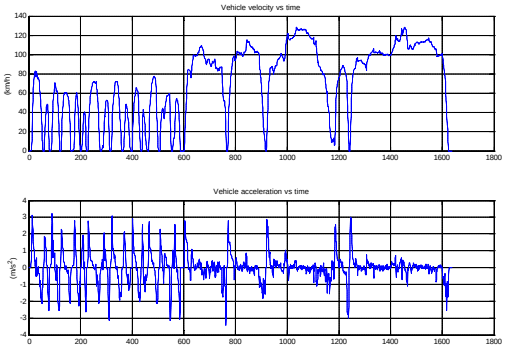

Fig.2: Air Resources board No.2 (ARB02) drive cycle.

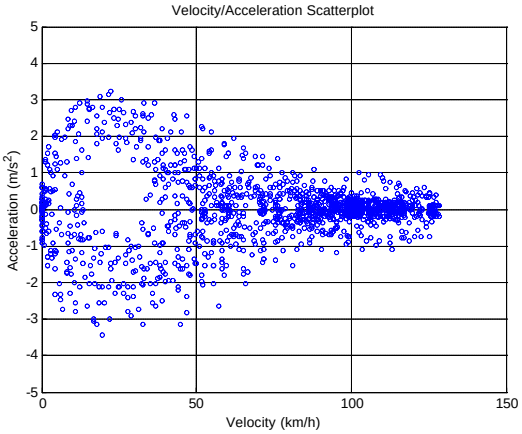

Fig.3: Scatter plot of speed vs. acceleration

Figure 2 shows the Air Resources board No.2 (ARB02) drive cycle. The plot contains both the speed profile vs. time the acceleration profile vs. time. The ARB02 is a cycle that contains both some city like driving and a period of highway cruising. Figure 3 shows a scatter plot of the ARB02 drive cycle indicating the range and distribution of time spent under various speeds and accelerations. The plot that is the key to understanding how a motors efficiency profile should be tuned to increase cycle efficiency is seen in figure 4. This plot shows the energy throughput at various torque levels and when combined with figure 3 it can be seen that the majority of the energy consumed occurs at low torque levels.

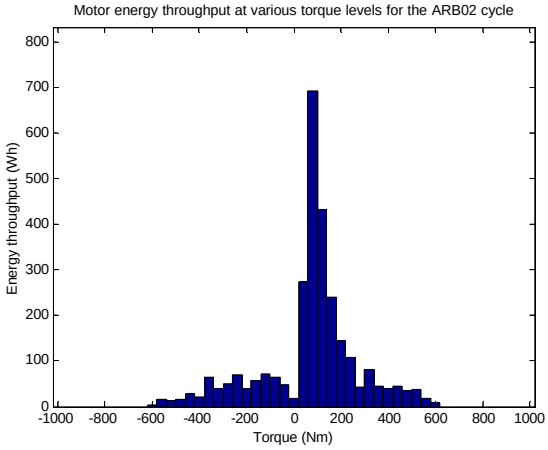

Fig.4: Histogram of energy through the motor vs. torque

Therefore, for high operational efficiency a drive motor in the UltraCommuter is required to have high efficiency at low torques over a wide speed range. When considering motor design this requirement translates to a motor with low no-load losses (i.e. low spinning losses).

4. IRONLESS MOTORS

Rare Earth Permanent Magnet Motors are regarded as the most appropriate choice of motors for direct wheel drive motors. A permanent magnet motor topology that has almost zero no-load losses is the Permanent Magnet Ironless motor [5, 6, 7, 8]. These motors have no iron in the stator and hence the only losses present in the core are conduction losses and eddy current losses in the copper.

5. BASIC MOTOR REQUIREMENTS

For the UltraCommuter there are a number of constraints that need to be meet by the drive system. These requirements are made up of performance requirements and of various system constraints.

The first requirement is that the motor must fit within the rear 17” wheel rims, this corresponds to outer diameter of the case of less than 390mm. The second constraint is that the motor should not add excessive unsprung mass to the rear wheel and so it was decided that a final cased motor should not weigh more than 25kg. The next requirements for the motor are so that the UltraCommuter can meet its performance requirements. The motor should be able to provide 500Nm peak torque for 5 second intervals and 250Nm for upward of 3 minutes. A top speed 1300RPM is required for a vehicle top speed of 150km/hr.

Motor Case Outside Diameter	390mm
Maximum RPM	1300
Peak Torque (10 sec)	500Nm
Sustained Torque (+3 minute)	250Nm
Maximum Motor Mass	25kg

Table 1: Basic Requirements

6. BASIC SIZING EQUATIONS

The following basic sizing equations can be used to develop an ironless motor concept. They are extremely simple and provide a rapid method of approximately sizing the motor. The equations assume a sinusoidal voltage and current input [8].

$$Torque = rBIL = \frac{1}{2} rB_{peak} J_{peak} V_{active} \quad (1)$$

$$P_{ResistiveLoss} = I^2 R = J_{rms}^2 V_{active} K_{ends} r \quad (2)$$

$$P_{EddyLoss} = \frac{pB_{peak}{}^2 w^2 D^4 L_{active} N_{conductors}}{128 r} \quad (3)$$

Equations (1), (2) & (3) lead to two basic equations stating the power output (4) and the total overall power loss (5). Equations (4) & (5) can be simply combined in different ways to provide losses in terms of torque and speed or efficiency at various torque and speeds.

$$P_{output} = \frac{1}{2} rB_{peak} J_{peak} V_{active} w \quad (4)$$

$$P_{loss} = \left(\frac{J_{peak}^2 K_{ends} r}{2} + \frac{B_{peak}^2 w^2 D^2}{32 r}\right) V_{active} \quad (5)$$

In order to use these equations some initial values must be able to be assumed as will be outlined.

6.1 Thermal Design Considerations

One of the major concerns with an ironless motor is the removal of heat from the stator. Ironless motors have very low inductance, meaning that for a given increase in current there is only a small change in air gap flux. The low inductance leads to almost no possibility of magnet demagnetization due to peak operating currents. This means that as long as the heat generated from conduction losses can be removed there is virtually no limit to the torque produced. However, as the torque is doubled the conduction losses increase by a factor of four. Cooling and thermal mass becomes a critical part of the final design to allow for transient acceleration torques of up to 500Nm.

For continuous operation thermal analysis becomes much more involved as the winding encapsulate, air temperature, surface air speed and even surface roughness comes into play. For automotive use the transient consideration far outweigh the continuous requirements. Figure 5 is a graph of the temperature rise of stator energized by various sinusoidal current densities. The figure assumes that the stator is only made of copper and that all heat generated is absorbed by the thermal mass of the copper and no heat escapes through cooling mechanisms. For the stators of the UltraCommuter a peak current density of 28Amps/m^2 was chosen.

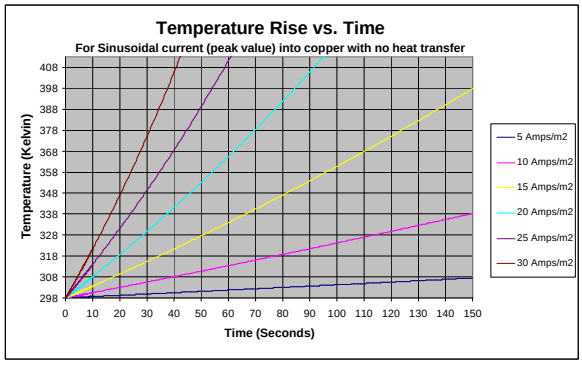

Fig.5: Temperature rise vs. time for various J (Amps/m^2)

6.2 Volume calculation for axial flux motor

The active volume (V_{active}) of a motor is defined in this paper as the copper volume that lies within the magnetic field (6). The total copper volume is then this active volume multiplied by a factor to take into account the end turns (K_{ends}) (7). Equation 8 is used to determine the average torque radius for an axial flux motor.

$$V_{active} = 2pR_{inner}(R_{outer} - R_{inner})t_{thickness} \quad (6)$$

$$K_{ends} = \frac{p(R_{outer} + R_{inner} + 4t_{thickness})}{N_{pole}(R_{outer} - R_{inner})} \quad (7)$$

$$r = \frac{(R_{outer} + R_{inner})}{2} \quad (8)$$

To this point the copper in the stator has been assumed to be basically solid, without insulation or empty voids. In determining the magnetic pole geometry it is essential that the actual volume of the stator be calculated and the running clearances of the motor determined.

6.2.1 Litz Design

In Ironless motors the stator copper is exposed to the full magnetic field and so in order to avoid excessive eddy currents in the windings Litz wire is used. Litz wire is a bundle of individually insulated fine wire used to replace a single conductor. Litz Wire was originally developed to reduce skin effect resistive losses in high frequency applications, where current in a conductor concentrates towards the surface of the conductor. In the design of an ironless motor the nominal wire diameter (D) affects

both the eddy current losses and the copper fill factor in the stator. As the nominal wire diameter (D) of the individual strands making up the Litz wire is reduced so are the eddy current losses, but so too is the copper fill factor.

A useful equation for the design of Litz wire has been determined by the company Wiretronic Inc. [9]. The equation (9) determines the overall diameter (OD) of a bundle Litz given the diameter of the individual wires including insulation ($D_{insulated}$) and the total number of wires (N).

$$OD = 1.155 D_{insulated} \sqrt{N} \qquad (9)$$

From equation (9) it is possible to determine fill factor for various wire diameters. Fill Factor can be defined as the actual copper volume divided by the total volume taken up by the wire. This can be determined by simply considering a cross-section of wire as in equation (10) were a circular bundle of Litz wire is placed in a square slot.

$$K_{fill} = \frac{pD^2}{5.34 D_{insulated}^2} \qquad (10)$$

A variation on equation (10) is where the fill factor is determined by assuming the litz wire bundle will be pressed square in the stator mould (11).

$$K_{fill} = \frac{D^2}{1.334 D_{insulated}^2} \qquad (11)$$

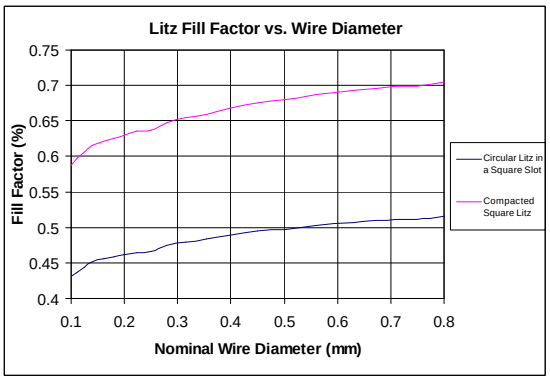

Fig. 6: Predicted Litz Fill factor vs. Nominal Wire Diameter

Figure 6 plots the change in fill factor for both equations (10) and (11) for Australian Standard wire diameters with single build insulation. For the UltraCommuter Stator a nominal wire diameter of 0.355mm was chosen with a single build PES insulation (Modified Polyurethane). PES insulation is able to withstand 163^0C temperatures for 20,000 hours and is the highest temperature solderable insulation commonly available in Australia. Litz wire can be supplied with an outer wrap (serving) of nylon or similar fiber to help hold the Litz bundle together. In this machine no outer serving was chosen as it further reduces fill factor, but depending on the winding method it may be necessary. One last point in determining the volume requirements of the stator is to consider the running clearance between the stator and the magnets – for this machine the clearance on each side of the stator was set to 1.5mm.

6.3 Magnetic Pole Design

The next step is to consider the magnetic pole geometry. This is the most difficult step in the design of a motor where many variables need to be taken into account. The primary consideration is the number of poles to be used in the motor. As the number of poles is increased the factor for the end turns K_{ends} (7) is reduced and so then too is the resistive power loss (2). Unfortunately there is also a trade-off – when the number of poles is increased so to is the flux leakage from one pole to another, which reduces the B_{peak}.

In order to take this into account a simple pole configuration was modeled as shown in fig 7. In order to allow this data to be used in various Ironless Motor designs it was decided to non-dimensionalise the magnetic pole and consider the two ratios of the Magnet Pole Width divided by the Magnet Thickness and Air Gap divided by the Magnet Thickness. Sixteen combinations were modeled to provide a rough guide to the peak flux density that might be expected given various pole geometries as seen in Fig.8. This data can be extrapolated to provide some points outside of the initial field of simulation.

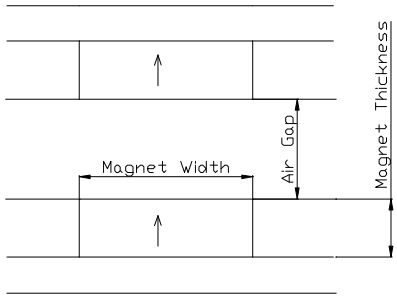

Fig. 7: Pole geometry for Non-dimensional Analysis

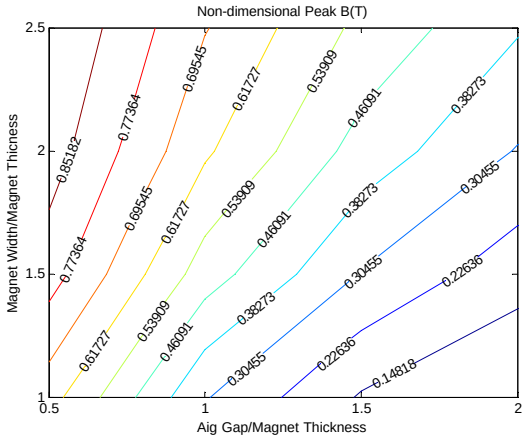

Fig. 8: Non-Dimensional Peak B (T) for Pole Geometry

6.4 Use of the basic Sizing Equations

A spreadsheet can now be used to step though the various configuration options, taking into account the considerations outlined above. As the variables are altered the efficiency of the motor can be calculated at various operating points and the mass of the magnets and the overall mass of motor can be considered.

The mass of the magnet backing iron reduces as the number of poles increase as the flux required to be turned reduces. The thickness of the backing iron is best calculated by FEA as not only the flux crossing the air-gap must be turned by the backing iron, but also the leakage flux. A rough initial estimate can be made by just considering the flux that crosses the air-gap and allowing a conservative flux of 1.2T in the backing Iron.

One interesting point to consider is when it is better to move from one to multiple stators in order to meet the toque requirement with a limited outer diameter. As the number of stators increases the magnetic pole geometry becomes more favorable, but so to does the air-gap volume taken up by the running clearances. In this particular case it was decided that two stators provided a good compromise of efficiency and complexity.

7. THE ULTRACOMMUTER WHEEL MOTOR

In the final stages of the design of the motor for the UltraCommuter various magnetic pole configurations were compared. This was in an effort to both reduce the magnetic mass and to provide a near sinusoidal flux density in the air-gap. The final configuration was a pair of axial flux stators with simplified Halbach Array on the outside and a plain magnet ring in the center.

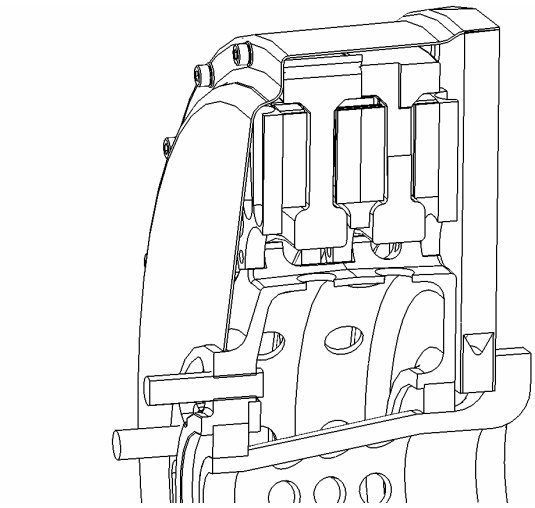

Fig 9. Cross section of the UltraCommuter Rear Wheel Mounted Direct Drive Motor

Figure 10 shows a cross-section through the average torque radius of the magnetic flux density B and figure 11 shows a plot of the flux density across the air-gap at the mid-plane of the air-gap.

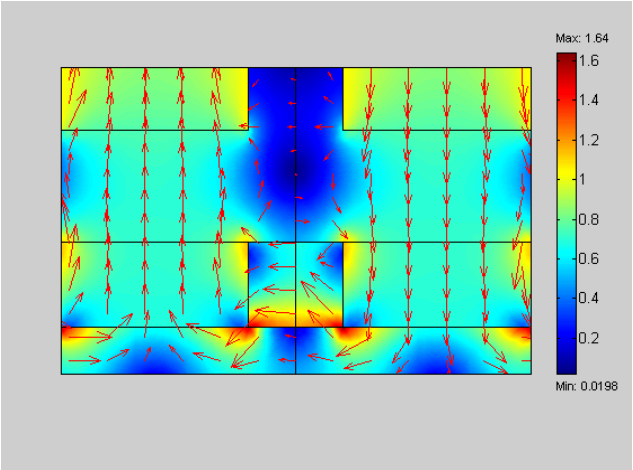

Fig. 10: Cross-section FEA plot of magnetic flux density

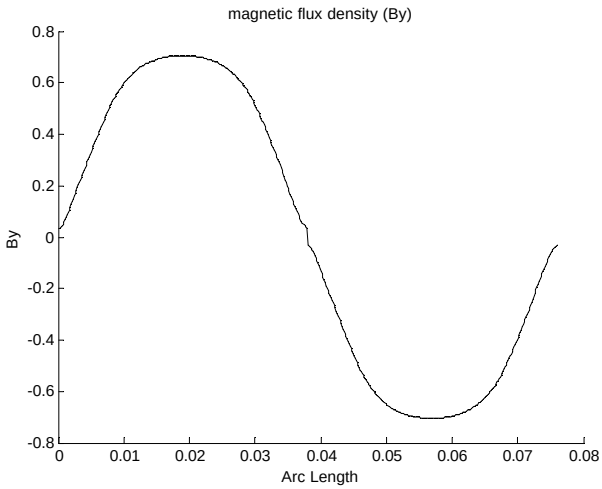

Fig. 11: Air Gap Flux Density

8. THE ULTRACOMMUTER DIRECT DRIVE WHEEL MOTOR

Number of Phases	3
Number of Poles	24 poles x 2 stators
Peak Air Gap Flux Density	0.65 T
Motor Case Outside Diameter	391mm
Peak Torque Continuous Torque	500Nm 250Nm
Magnet Mass Active mass (including magnets) Total motor mass	8.9 kg 18.3 kg 24 kg
Throughput cycle efficiency: Air Resources board No.2 (ARB02) Urban dynamometer drive cycle (UDDS) Highway Fuel economy test (HWFET)	 94.1% 92.6% 97.3%

Table 2: UltraCommuter Motor Specifications

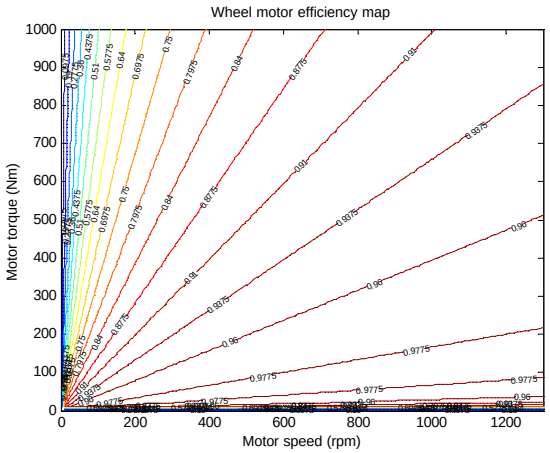

Fig. 12. Output efficiency of the two wheel motors combined to drive the UltraCommuter

As seen in Table 2 and Figure 12, the Ultracommuter direct drive wheel motor demonstrates that brushless ironless motors can produce extremely high torque densities (torque per unit mass) with appropriate design, and are not limited to high speed applications. Because of their very low spinning losses, efficiency at low torques and varying speeds is very high, ensuring high efficiency in their actual application as vehicle traction drives as measured using driving cycles.

The wheel motors are currently in the final stages of manufacture and experimental results will be presented in future publications.

9. REFERENCES

[1] Lovins, A.B., "Hypercars: The Next Industrial Revolution", 13th International Electric Vehicle Symposium (EVS-13), Osaka, Japan. 1996

[2] Simpson, A.G., Walker, G.R., Greaves, M.C., Finn, D., Guymer, B.D., "The UltraCommuter: A viable and Desirable Solar-Powered Commuter Vehicle", Australasian Universities Power Engineering Conference AUPEC'02, Melbourne, Australia. 2002.

[3] Simpson, A.G., Greaves, M.C., and Walker G.R., "Migrating to a sustainable energy system: Distributed Generation and storage, fuel cells and hypercars", AUPEC, Brisbane, Australia 2000. p. 289-94

[4] National Renewable Energy Laboratory – ADVISOR: http://ctts.nrel.gov/analysis/advisor.html

[5] Caricchi, F., Mezzetti, F., and Santini, E., "Multistage Axial-Flux PM Machine for Wheel Direct Drive", IEEE Transactions on Industrial Applications, Vol. 32, No. 4, July/August 1996.

[6] Caricchi, F., Crescimbini, F., Hororati, O., Baianco, G.L., and Santini, E., "Performance of Coreless-Winding Axial-Flux Permanent-Magnet Generator With Power Output at 400 Hz, 3000 r/min", IEEE Transactions on Industrial Applications, Vol. 34, No. 6, November/December 1998.

[7] Lovatt, H.C., Ramsden, V.S., and Mecrow, B.C., "Design of an in-wheel motor for a solar-powered electric vehicle", IEE Proc.-Electr. Power Appl, Vol. 145, No. 5, September 1998.

[8] Greaves, M.C., Walker, G.R., Walsh, B.B., "Design optimization of Ironless Motors based on magnet selection", Journal of Electrical & Electronics Engineering, Australia, IEAUST, vol. 21, no. 1, pp.49-56.

[9] WireTronic Inc: http://www.wiretron.com/litz.html

10. BIOGRAPHY

Matthew Greaves was born in Katoomba, Australia, in 1975. He received a B.E. degree (Mechanical Engineering) at the University of Queensland in 1996. During his degree he was the technical coordinator for the highly successful University of Queensland Sunshark solar vehicle team. During 1997, he was employed by Transport Energy Systems to work on the development of two hybrid electric buses. In 1998, he joined Velocity Engineering AG, located in Basel Switzerland, to develop a production version of their electric assisted bicycle. In 1999, he returned to the University of Queensland and took up an engineering position in the University's technology commercialisation company UniQuest Pty Ltd. He is currently in his 3rd year of a Ph.D. in the School of Information Technology and Electrical Engineering at the University of Queensland. His research focuses on wheel motors for electric and fuel cell vehicles, with a particular focus on ironless machines. He is also currently involved in the development of the UltraCommuter concept vehicle within the Sustainable Energy Research Group at the University of Queensland and is a partner is his own engineering firm, GWG Creative Engineering.